

# **Iron's impact on silicon solar cell execution: comprehensive modeling across diverse scenarios**

Oleg Olikh, Oleksii Zavhorodnii

*Taras Shevchenko National University of Kyiv, 64/13, Volodymyrska Street,  
Kyiv, 01601, Ukraine*

[olegolikh@knu.ua](mailto:olegolikh@knu.ua)

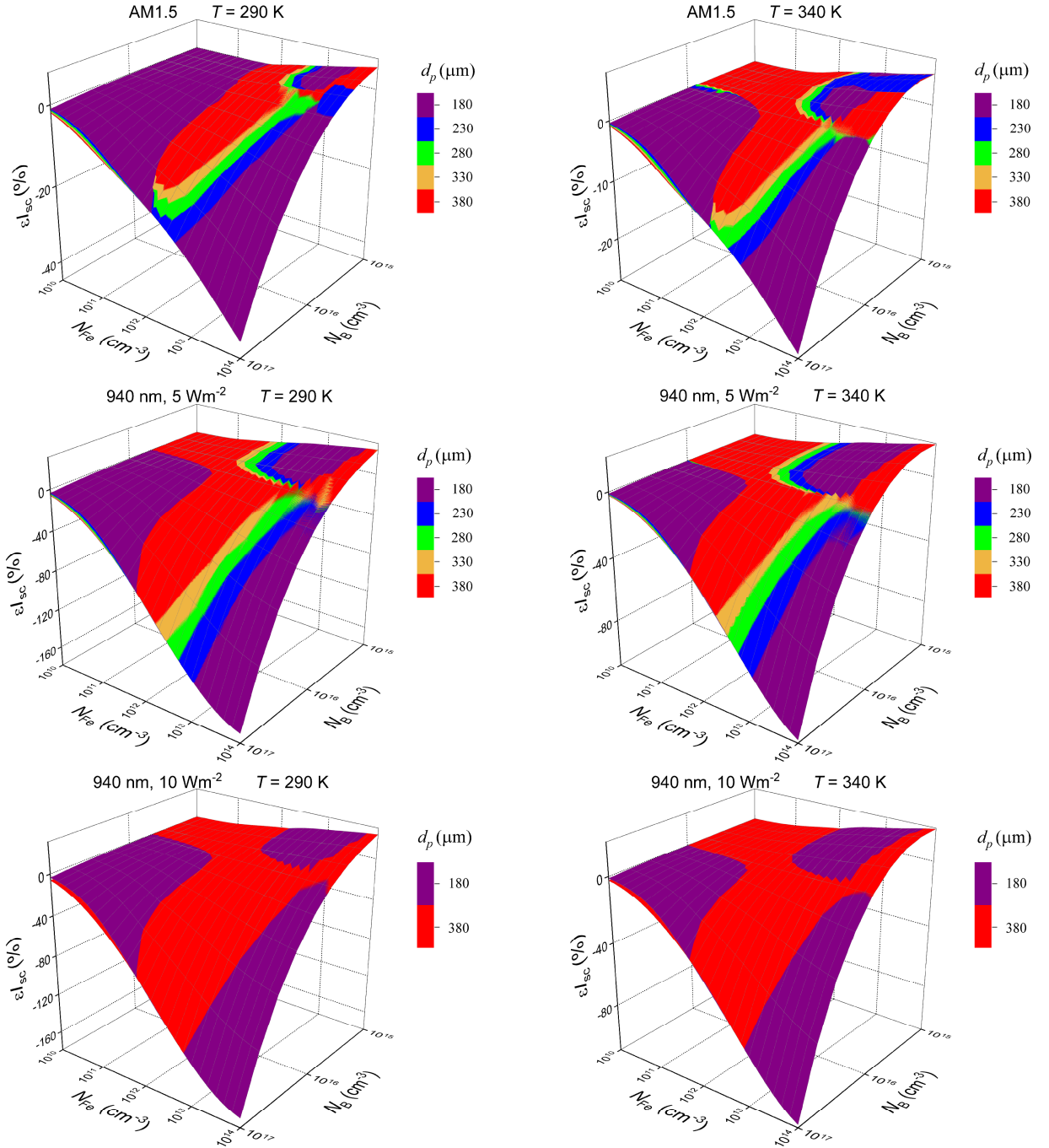


Fig.S1. Relative changes in short-circuit current caused by a complete dissociation of  $\text{Fe}_i\text{B}_s$  pairs as a function of iron concentration and doping level for SC with different base depth.  $T, \text{K}$ : 290 (left panels), 340 (right panels).

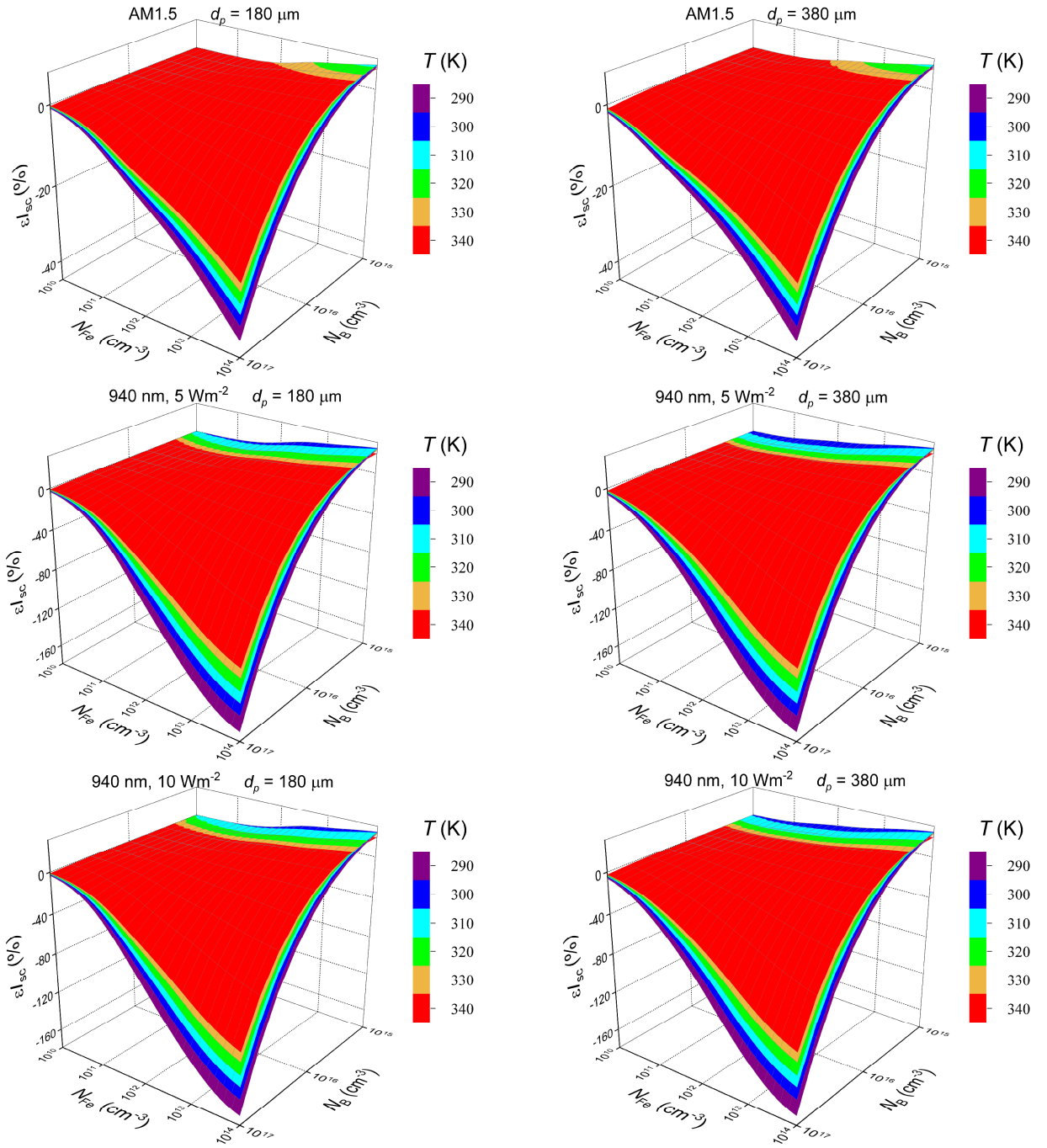


Fig.S2. Relative changes in short-circuit current caused by a complete dissociation of Fe<sub>i</sub>B<sub>s</sub> pairs as a function of iron concentration and doping level at different temperatures.  $d_p$ ,  $\mu\text{m}$ : 180 (left panels), 380 (right panels).

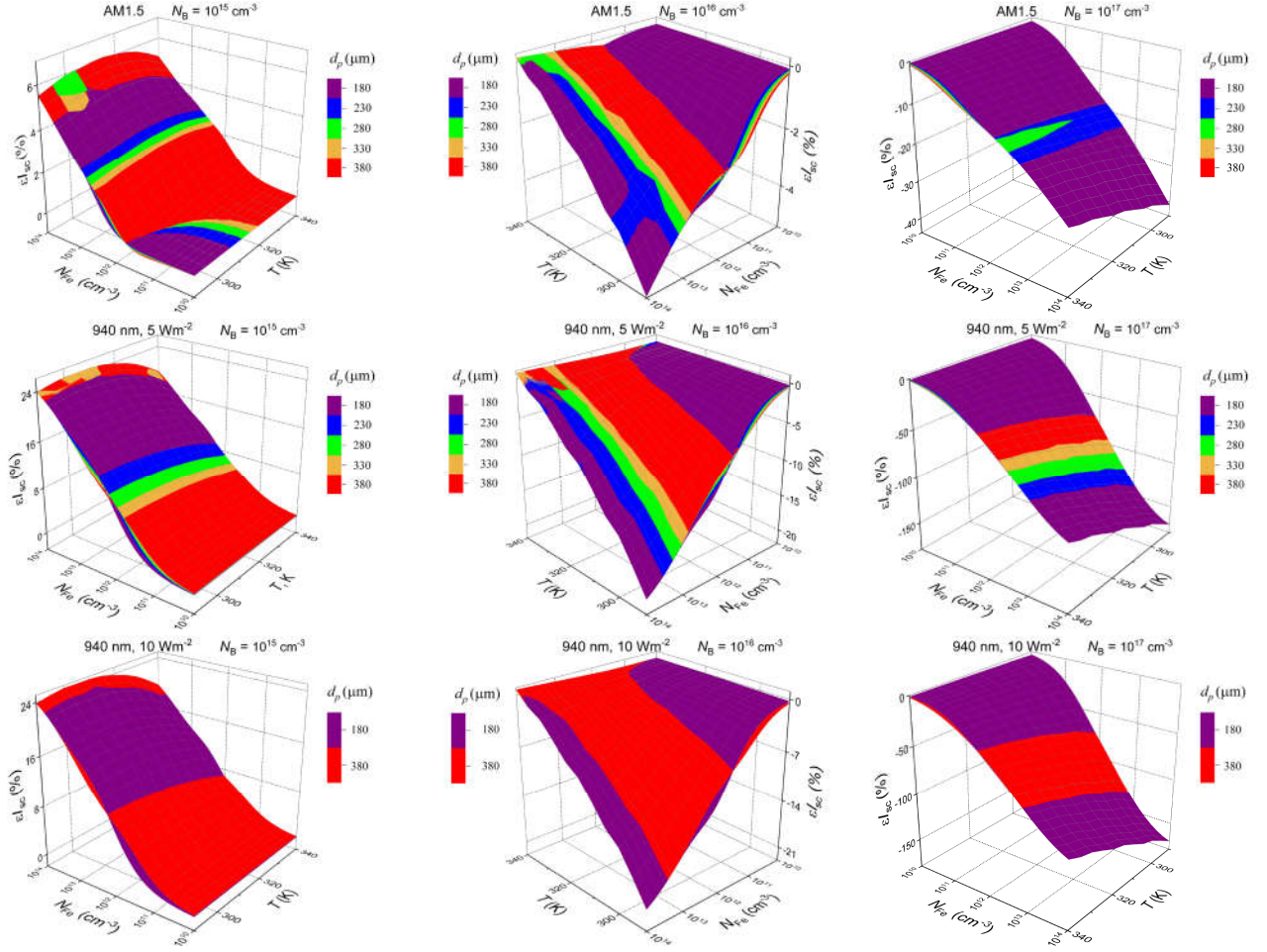


Fig.S3 Relative changes in short-circuit current caused by a complete dissociation of  $\text{Fe}_i\text{B}_s$  pairs as a function of iron concentration and temperature for SC with different base depth.  $N_B$ ,  $\text{cm}^{-3}$ :  $10^{15}$  (left panels),  $10^{16}$  (middle panels),  $10^{17}$  (right panels).

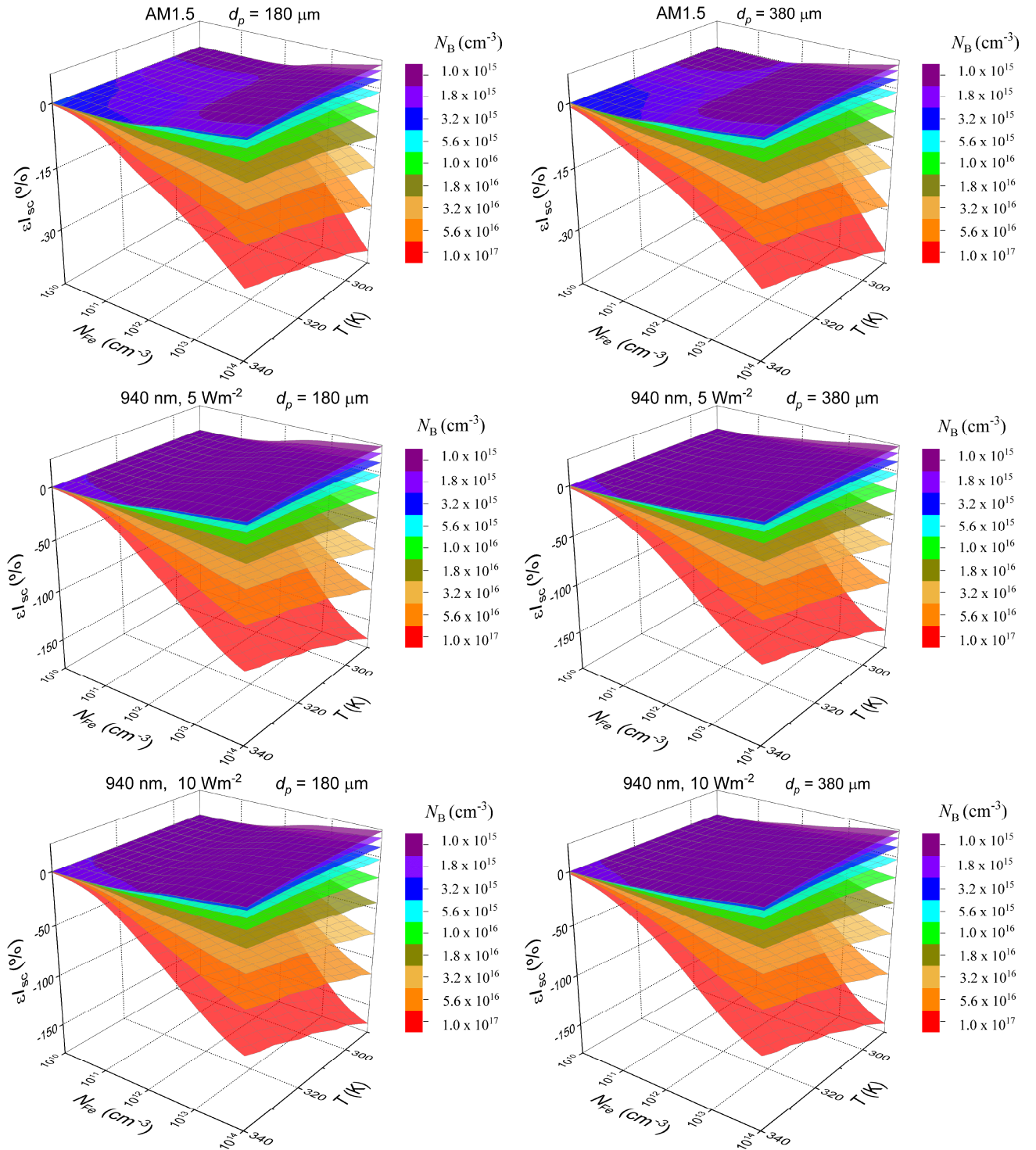


Fig.S4. Relative changes in short-circuit current caused by a complete dissociation of  $Fe_iB_s$  pairs as a function of iron concentration and temperature for SC with different base doping level.  $d_p$ ,  $\mu m$ : 180 (left panels), 380 (right panels).

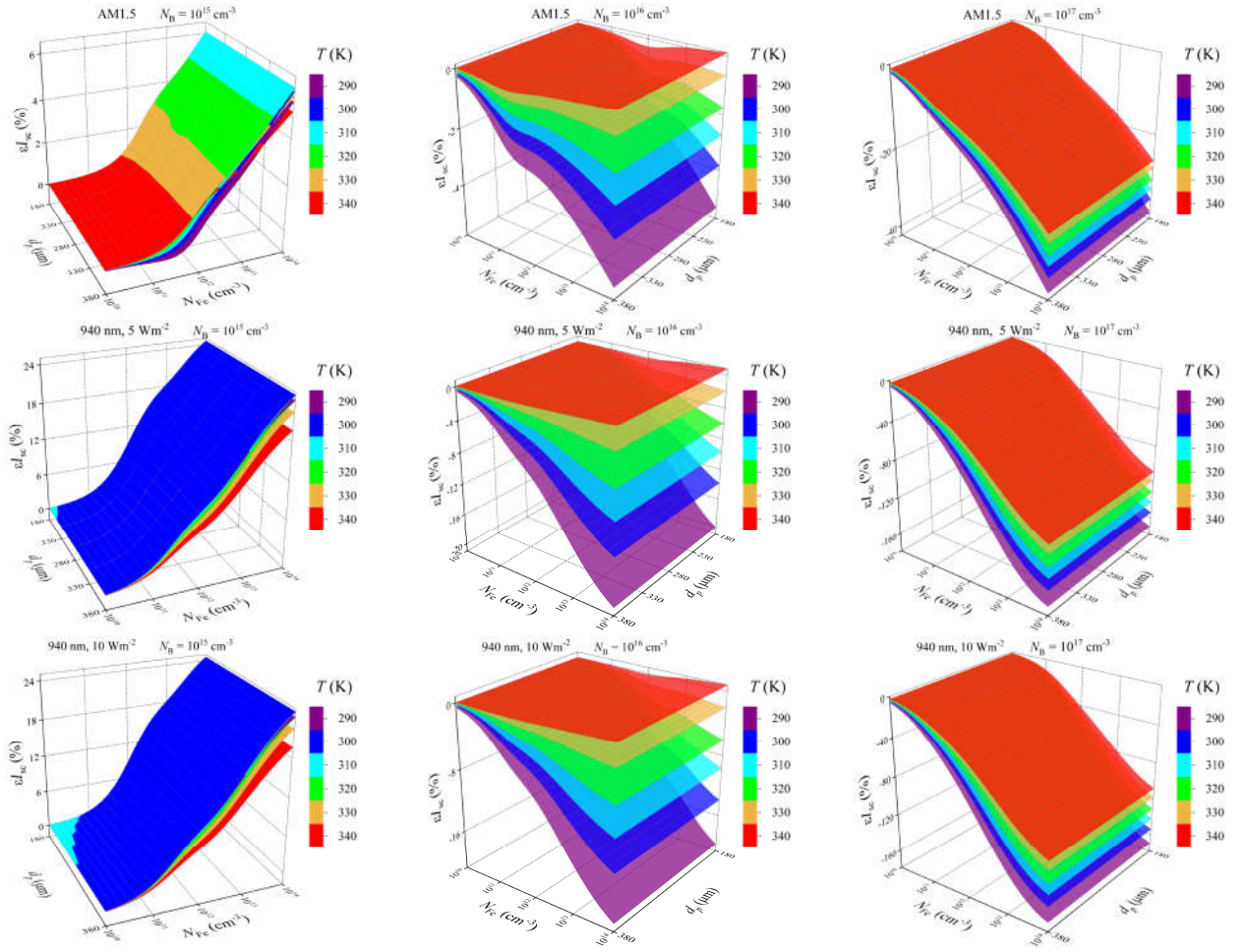


Fig.S5. Relative changes in short-circuit current caused by a complete dissociation of Fe<sub>i</sub>B<sub>s</sub> pairs as a function of iron concentration and base depth for different temperatures.  $N_B$ ,  $\text{cm}^{-3}$ :  $10^{15}$  (left panels),  $10^{16}$  (middle panels),  $10^{17}$  (right panels).

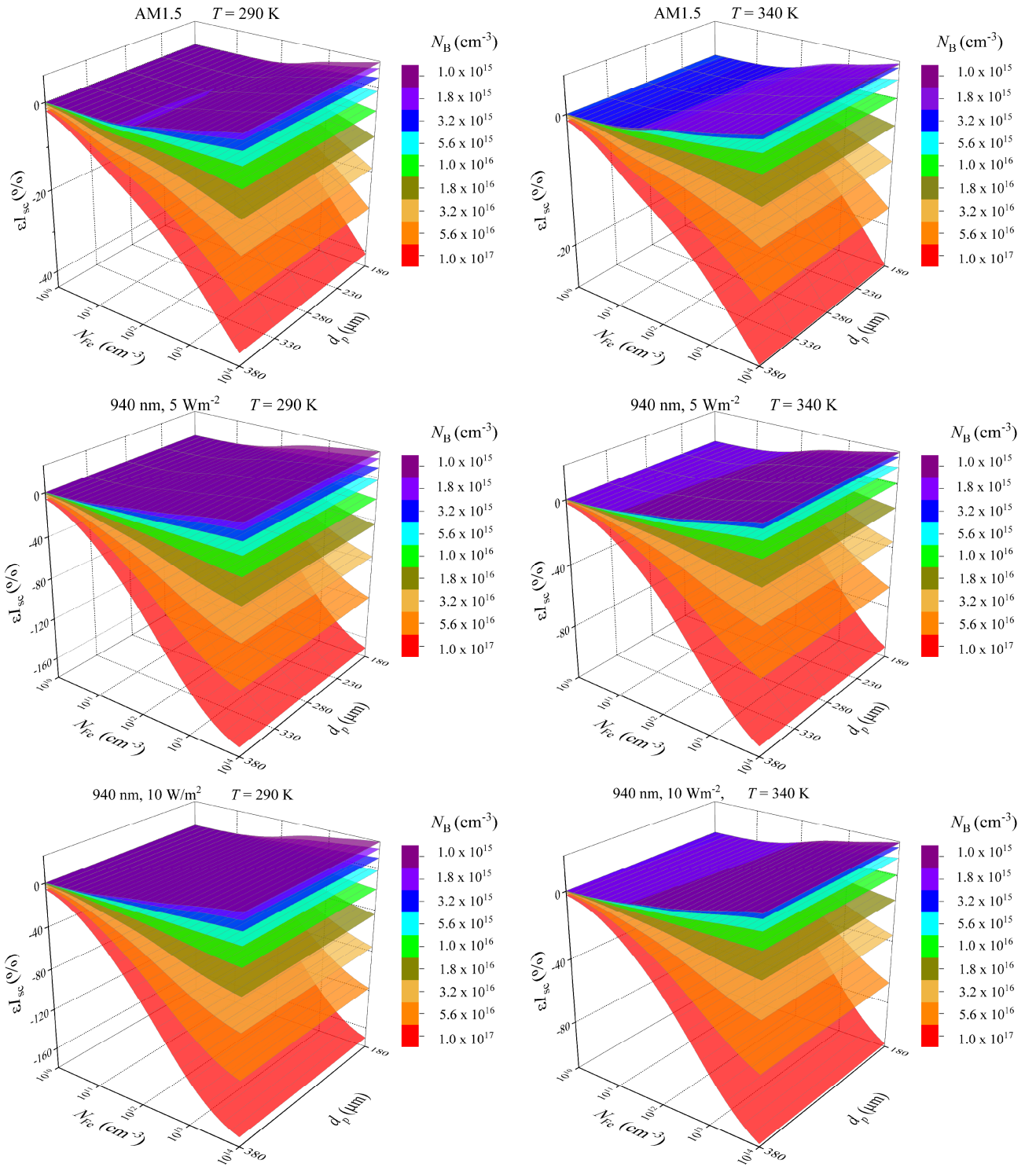


Fig.S6. Relative changes in short-circuit current caused by a complete dissociation of  $\text{Fe}_i\text{B}_s$  pairs as a function of iron concentration and base depth for SC with different base doping level.  $T, \text{K}$ : 290 (left panels), 340 (right panels).

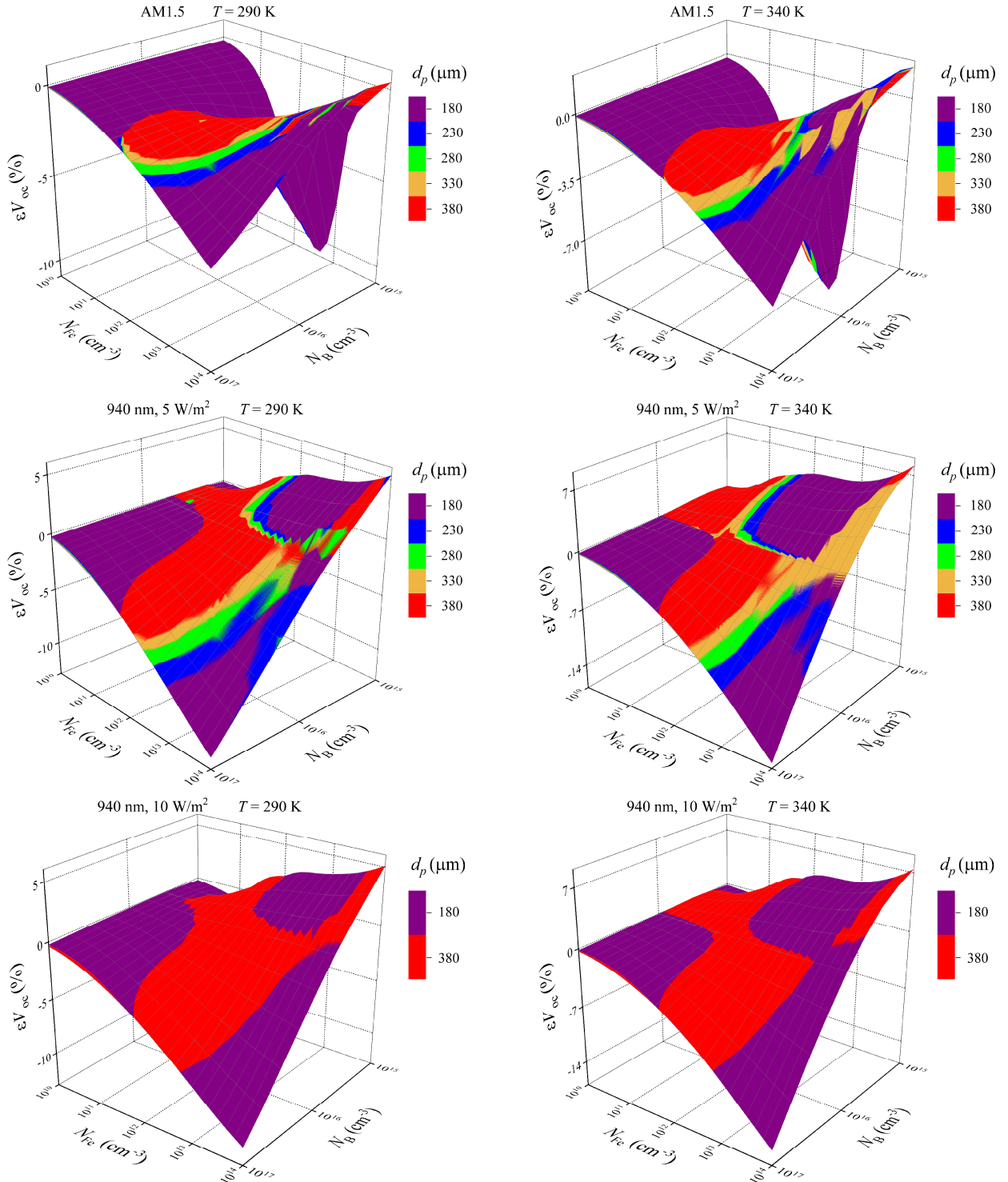


Fig.S7. Relative changes in open-circuit voltage caused by a complete dissociation of  $\text{Fe}_i\text{B}_s$  pairs as a function of iron concentration and doping level for SC with different base depth.  $T, \text{K}$ : 290 (left panels), 340 (right panels).

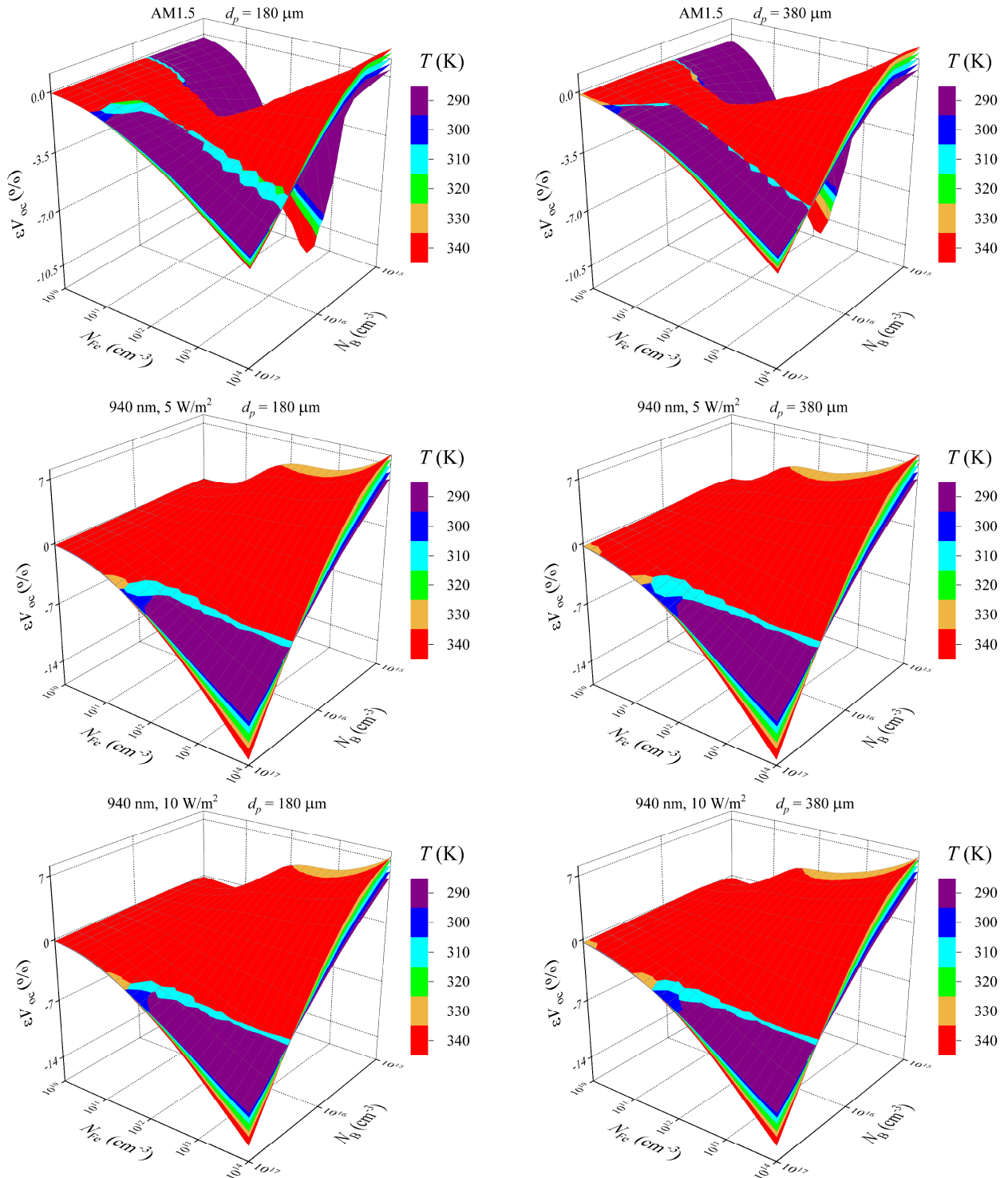


Fig.S8. Relative changes in open-circuit voltage caused by a complete dissociation of  $\text{Fe}_i\text{B}_s$  pairs as a function of iron concentration and doping level at different temperatures.  $d_p$ ,  $\mu\text{m}$ : 180 (left panels), 380 (right panels).

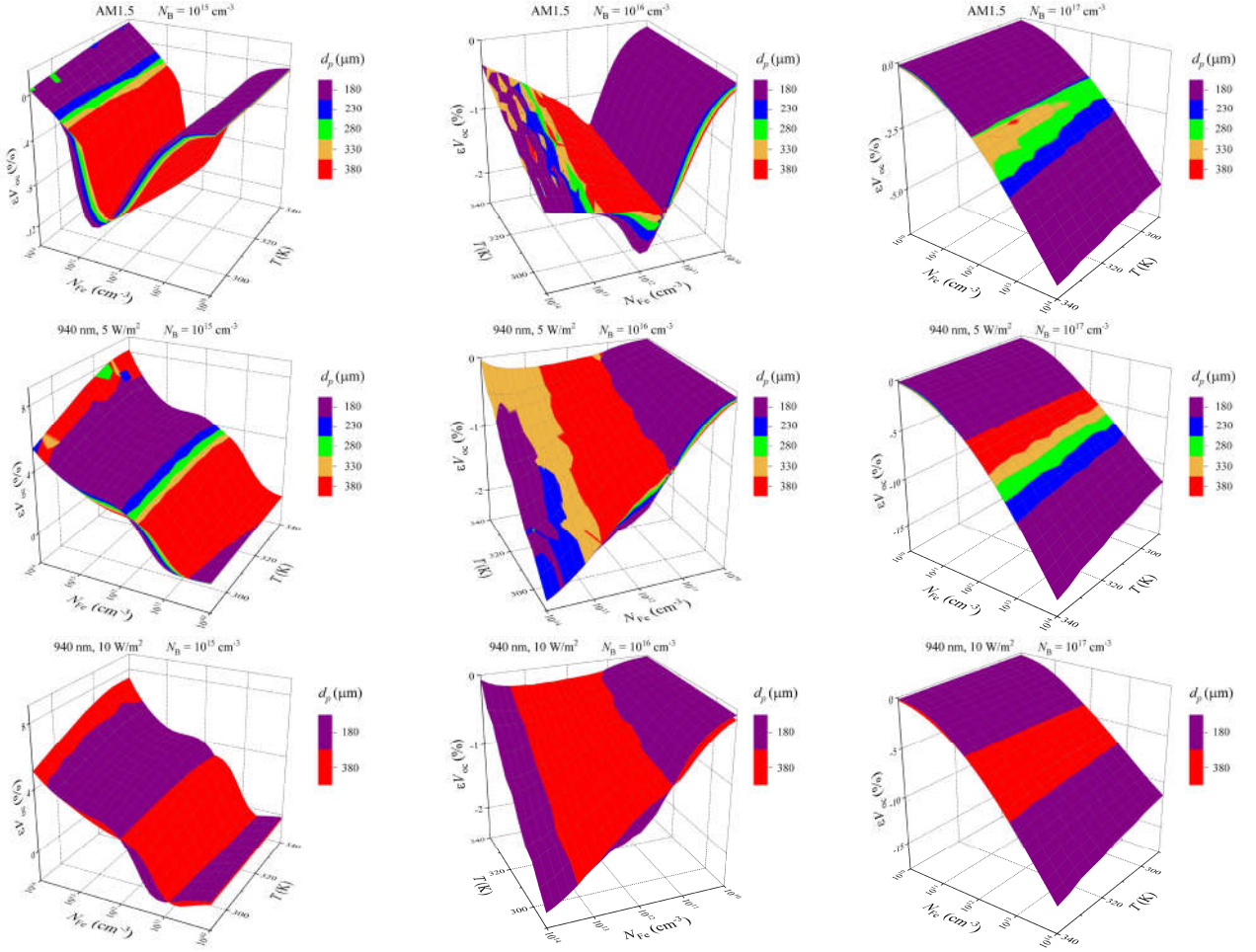


Fig.S9. Relative changes in open-circuit voltage caused by a complete dissociation of Fe<sub>i</sub>B<sub>s</sub> pairs as a function of iron concentration and temperature for SC with different base depth.  $N_B$ ,  $\text{cm}^{-3}$ :  $10^{15}$  (left panels),  $10^{16}$  (middle panels),  $10^{17}$  (right panels).

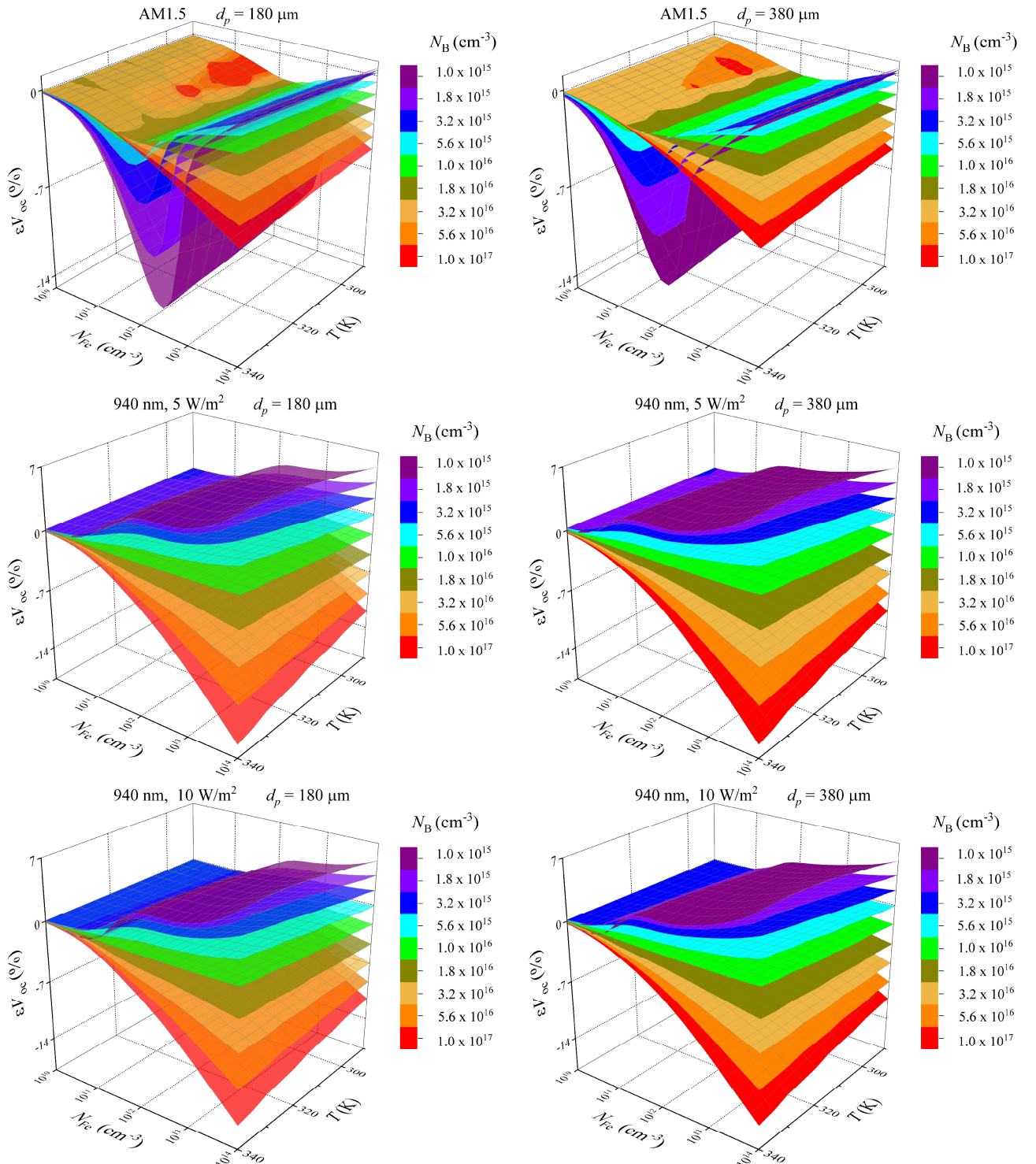


Fig.S10. Relative changes in open-circuit voltage caused by a complete dissociation of  $\text{Fe}_i\text{B}_s$  pairs as a function of iron concentration and temperature for SC with different base doping level.  $d_p$ ,  $\mu\text{m}$ : 180 (left panels), 380 (right panels).

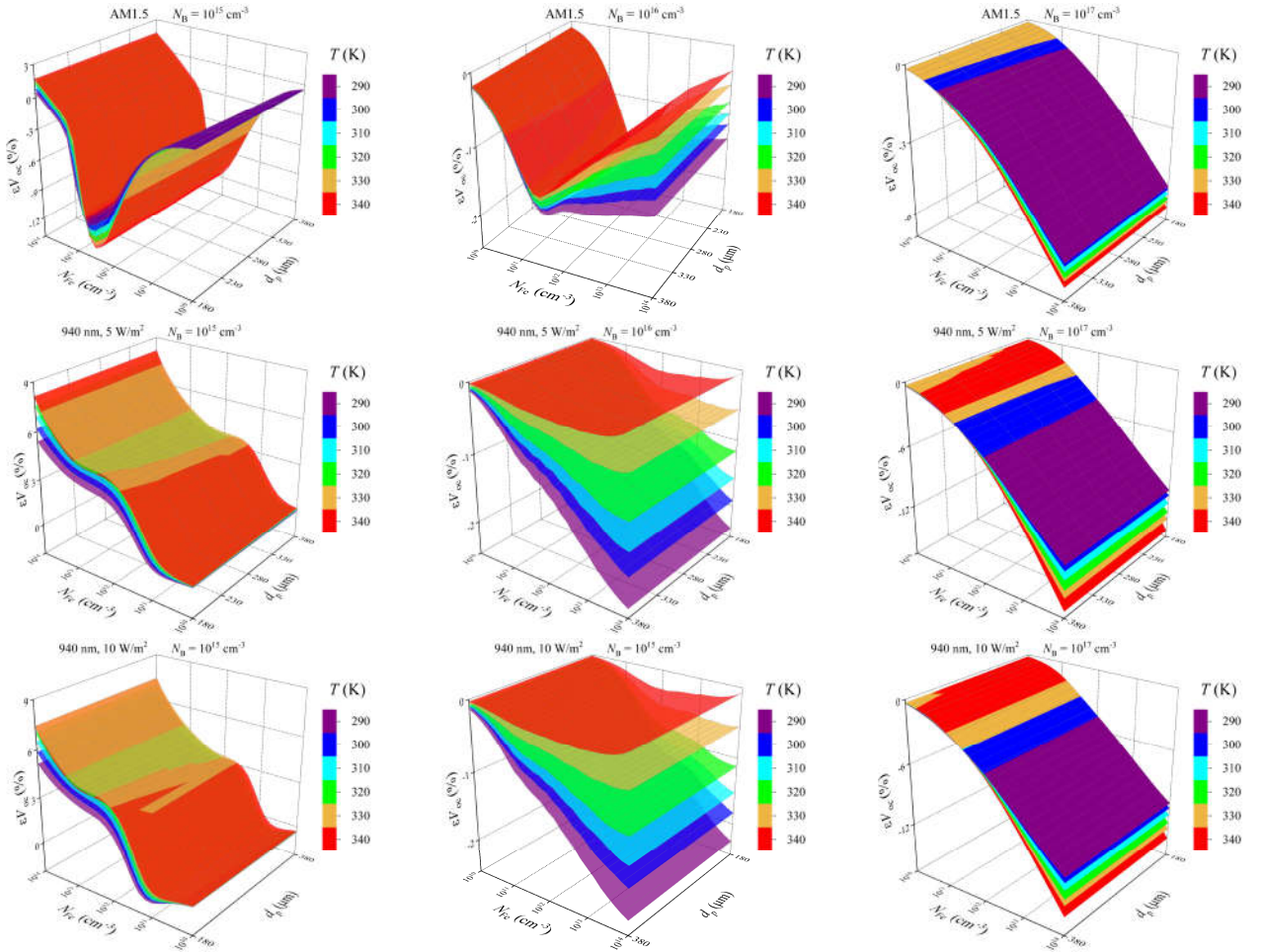


Fig.S11. Relative changes in open-circuit voltage caused by a complete dissociation of  $\text{Fe}_i\text{B}_s$  pairs as a function of iron concentration and base depth for different temperatures.  $N_B$ ,  $\text{cm}^{-3}$ :  $10^{15}$  (left panels),  $10^{16}$  (middle panels),  $10^{17}$  (right panels).

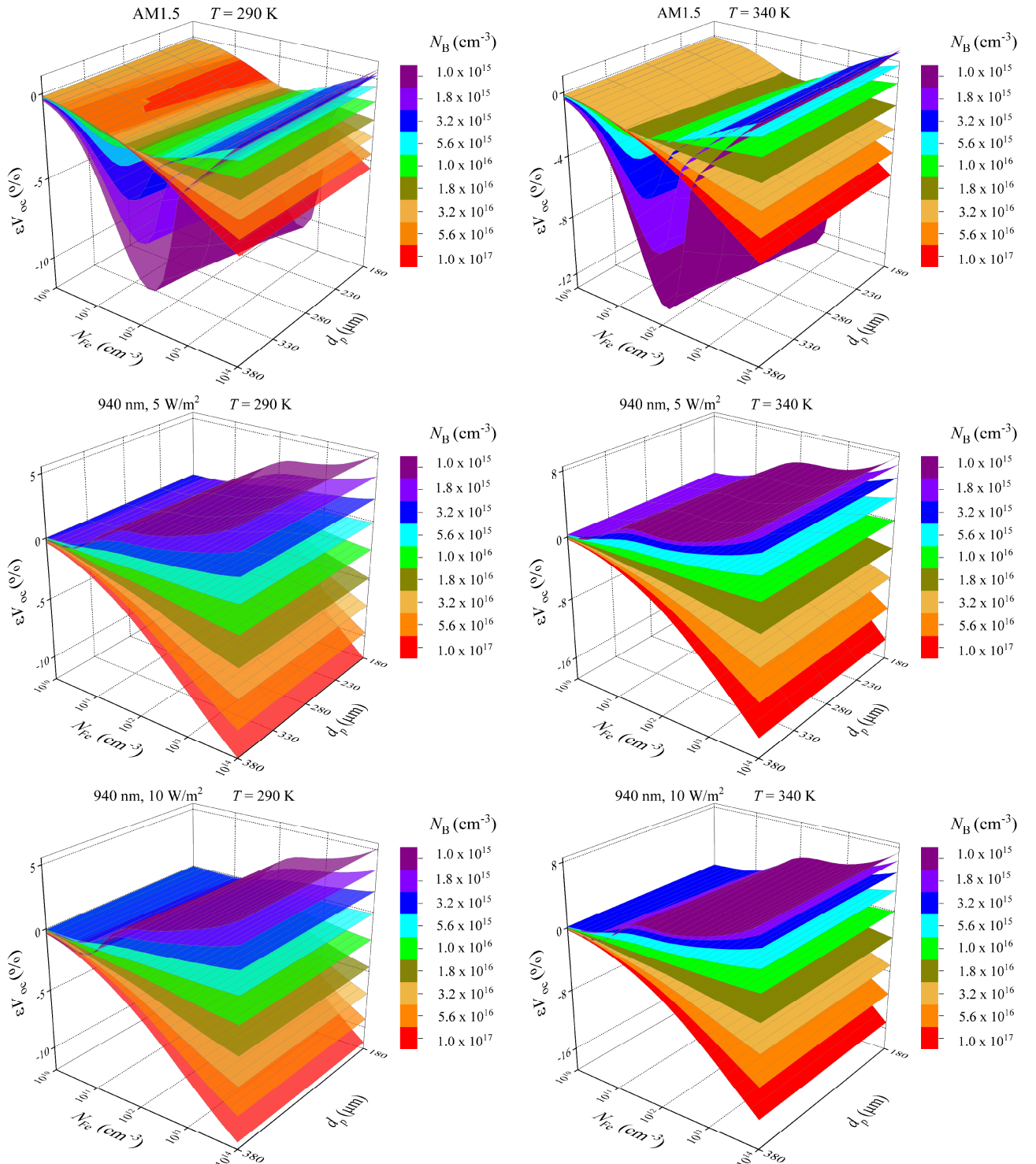


Fig.S12. Relative changes in open-circuit voltage caused by a complete dissociation of  $\text{Fe}_i\text{B}_s$  pairs as a function of iron concentration and base depth for SC with different base doping level.  $T, \text{K}$ : 290 (left panels), 340 (right panels).

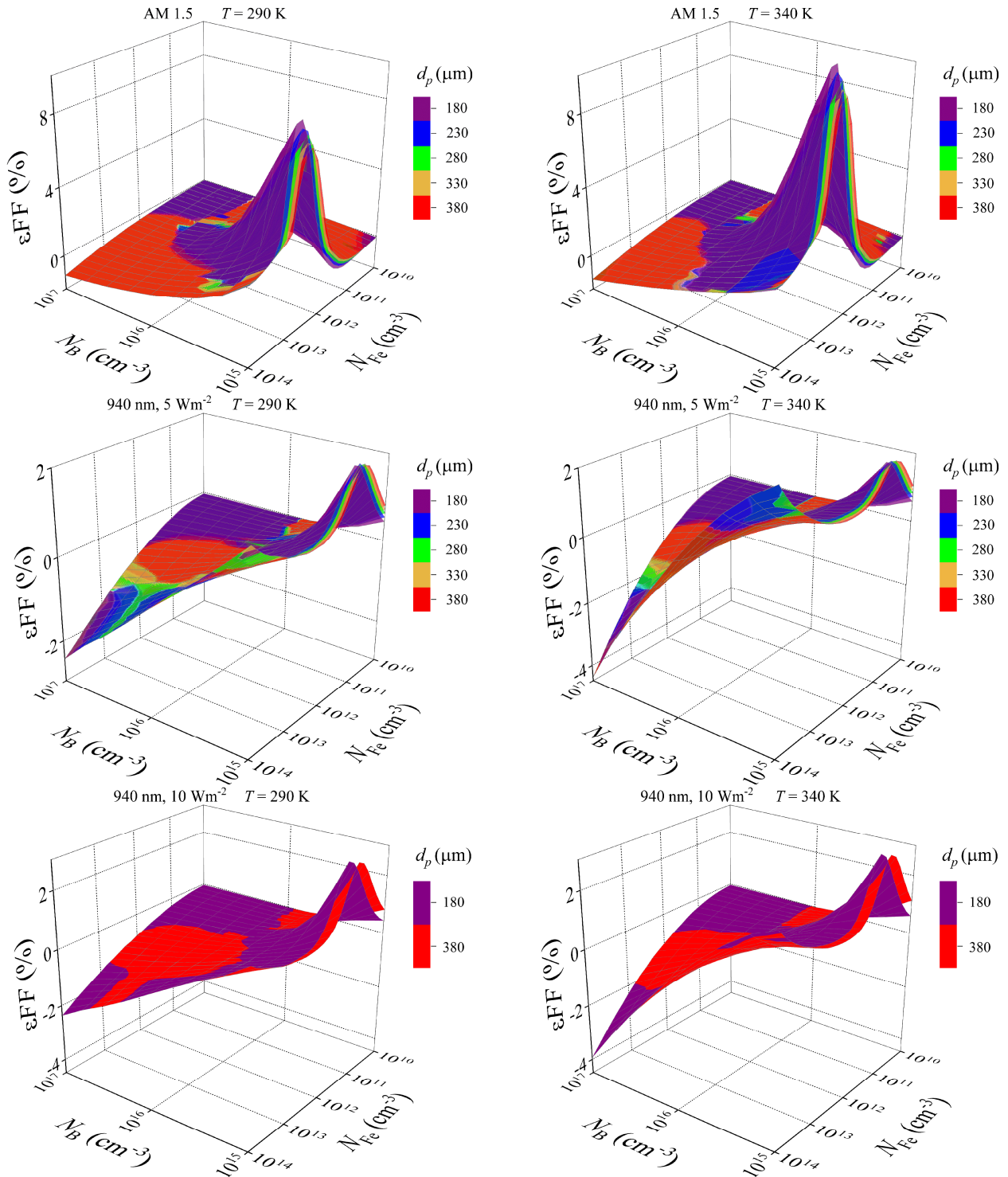


Fig.S13. Relative changes fill factor caused by a complete dissociation of  $\text{Fe}_i\text{B}_s$  pairs as a function of iron concentration and doping level for SC with different base depth.  $T, \text{K}$ : 290 (left panels), 340 (right panels).

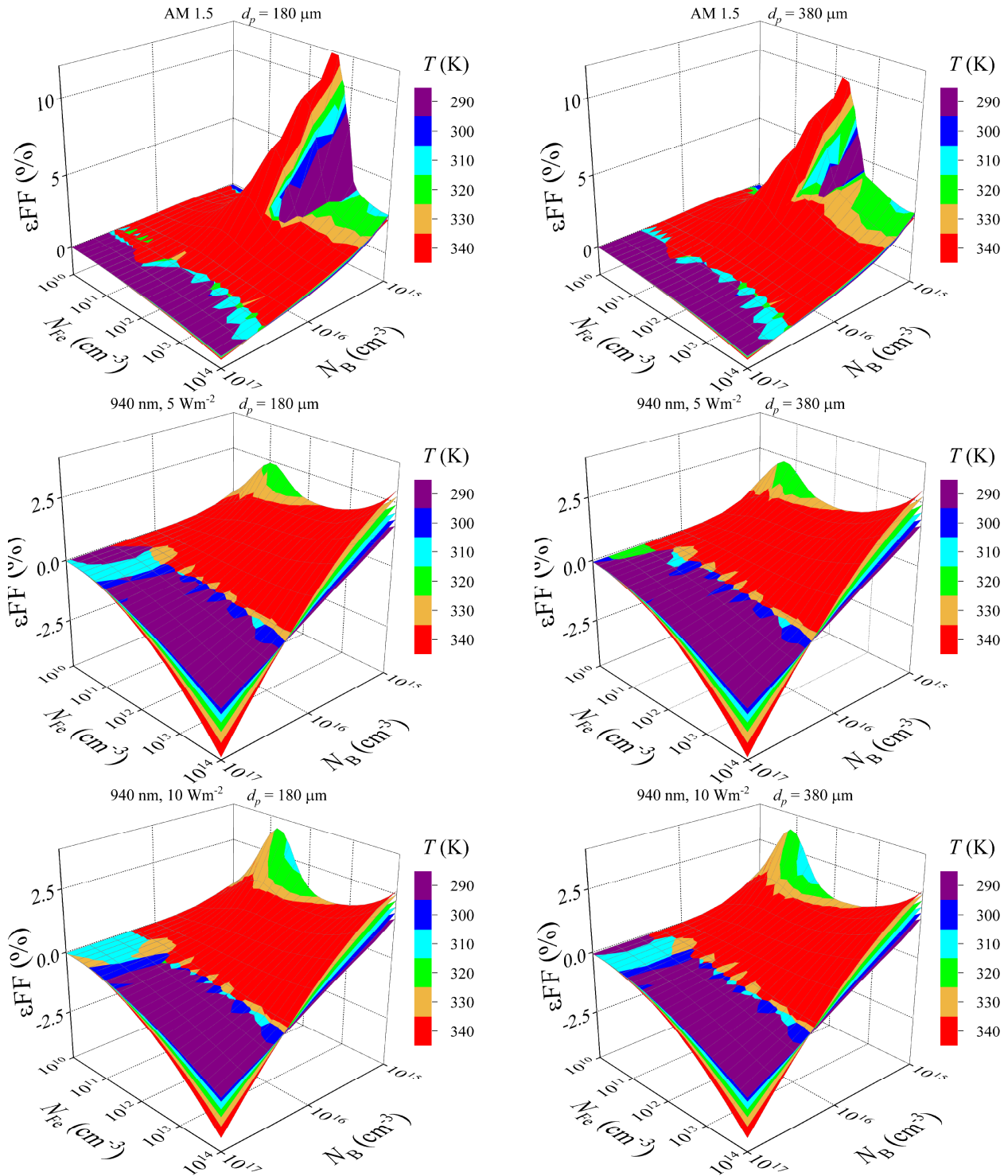


Fig.S14. Relative changes fill factor caused by a complete dissociation of  $\text{Fe}_i\text{B}_s$  pairs as a function of iron concentration and doping level at different temperatures.  $d_p$ ,  $\mu\text{m}$ : 180 (left panels), 380 (right panels).

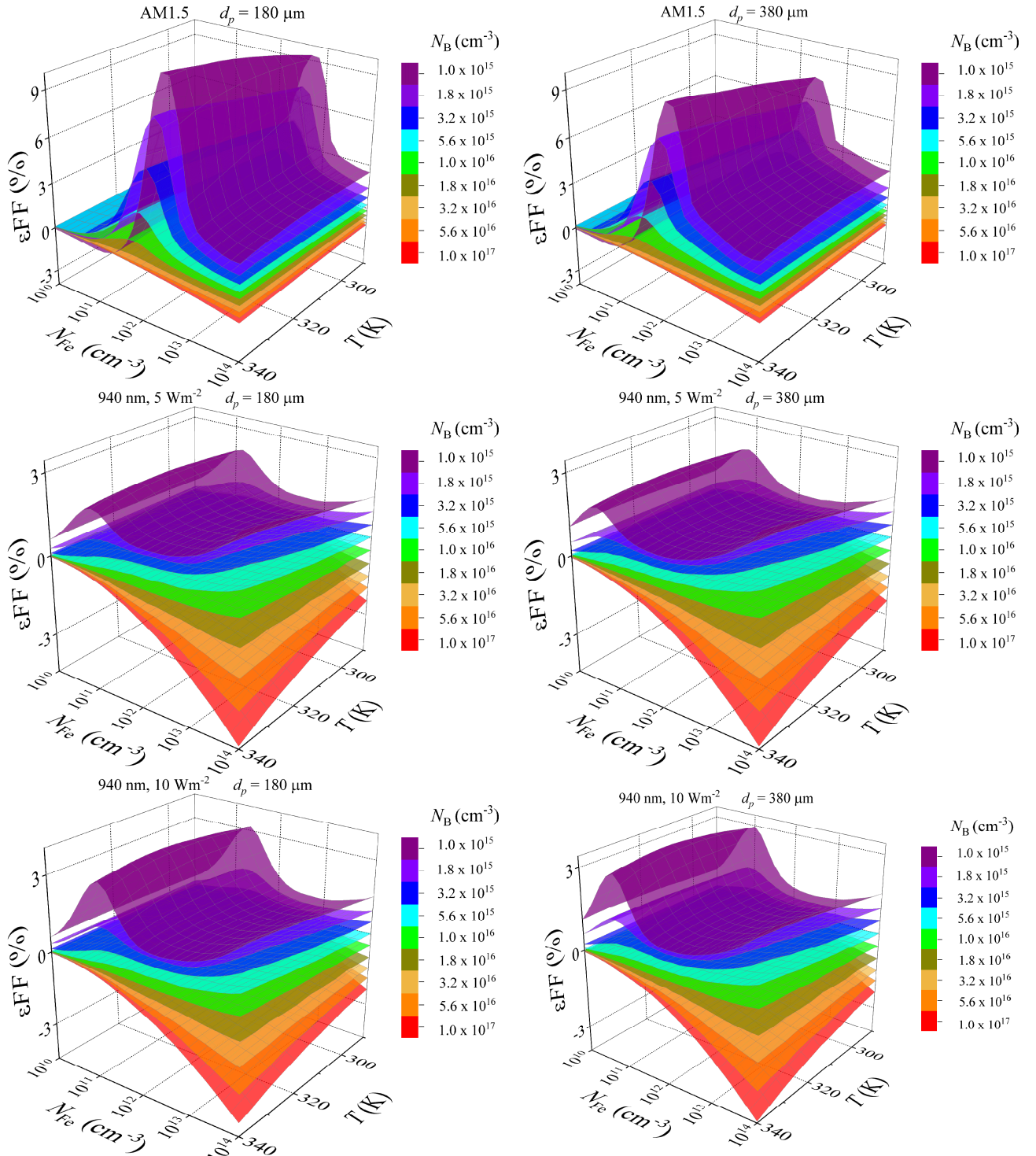


Fig.S15. Relative changes in fill factor caused by a complete dissociation of  $\text{Fe}_1\text{B}_8$  pairs as a function of iron concentration and temperature for SC with different base doping level.  $d_p$ ,  $\mu\text{m}$ : 180 (left panels), 380 (right panels).

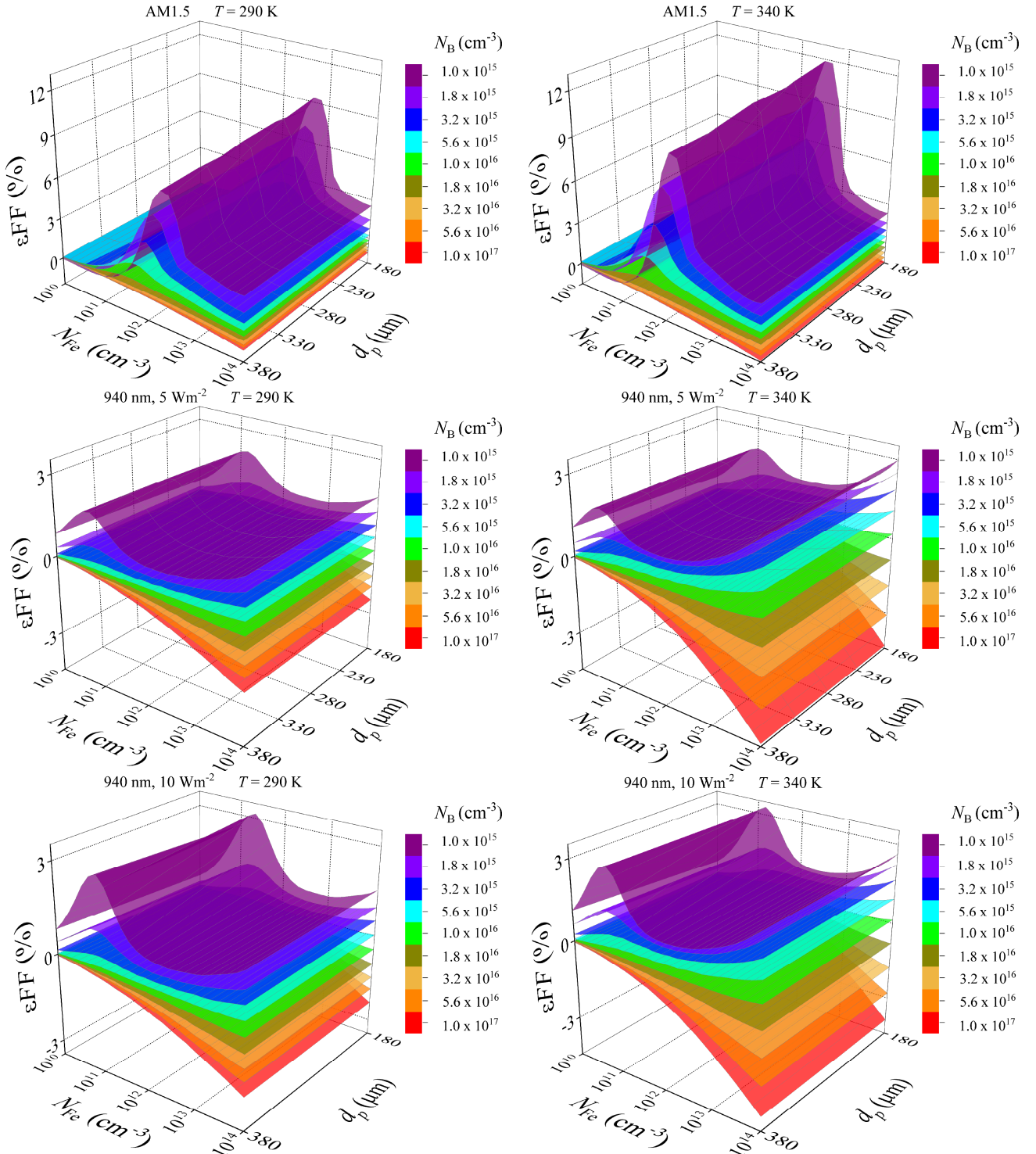


Fig.S16. Relative changes in fill factor caused by a complete dissociation of  $\text{Fe}_i\text{B}_s$  pairs as a function of iron concentration and base depth for SC with different base doping level.  $T, \text{K}$ : 290 (left panels), 340 (right panels).

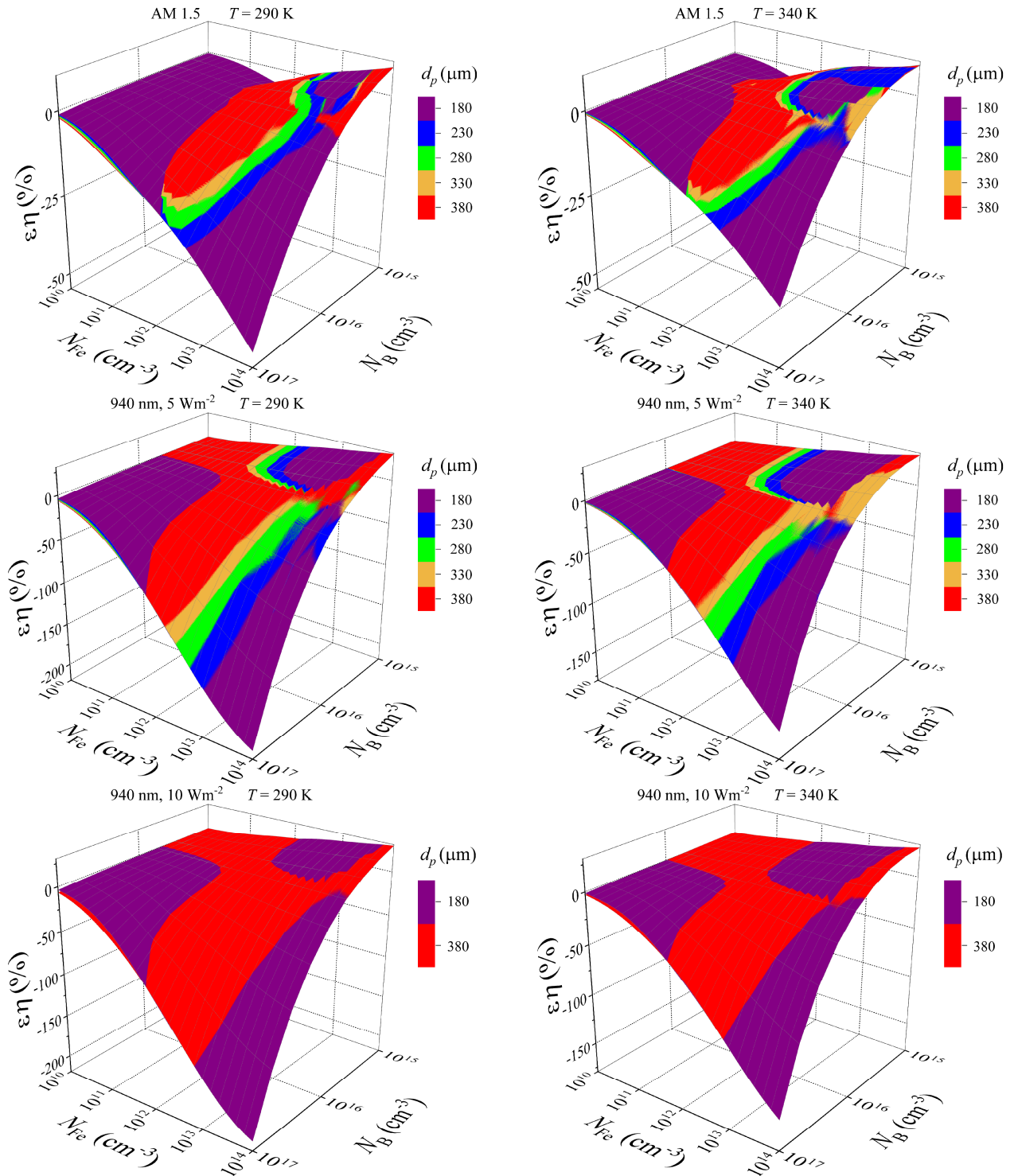


Fig.S17. Relative changes efficiency caused by a complete dissociation of  $\text{Fe}_i\text{B}_s$  pairs as a function of iron concentration and doping level for SC with different base depth.  $T, \text{K}$ : 290 (left panels), 340 (right panels).

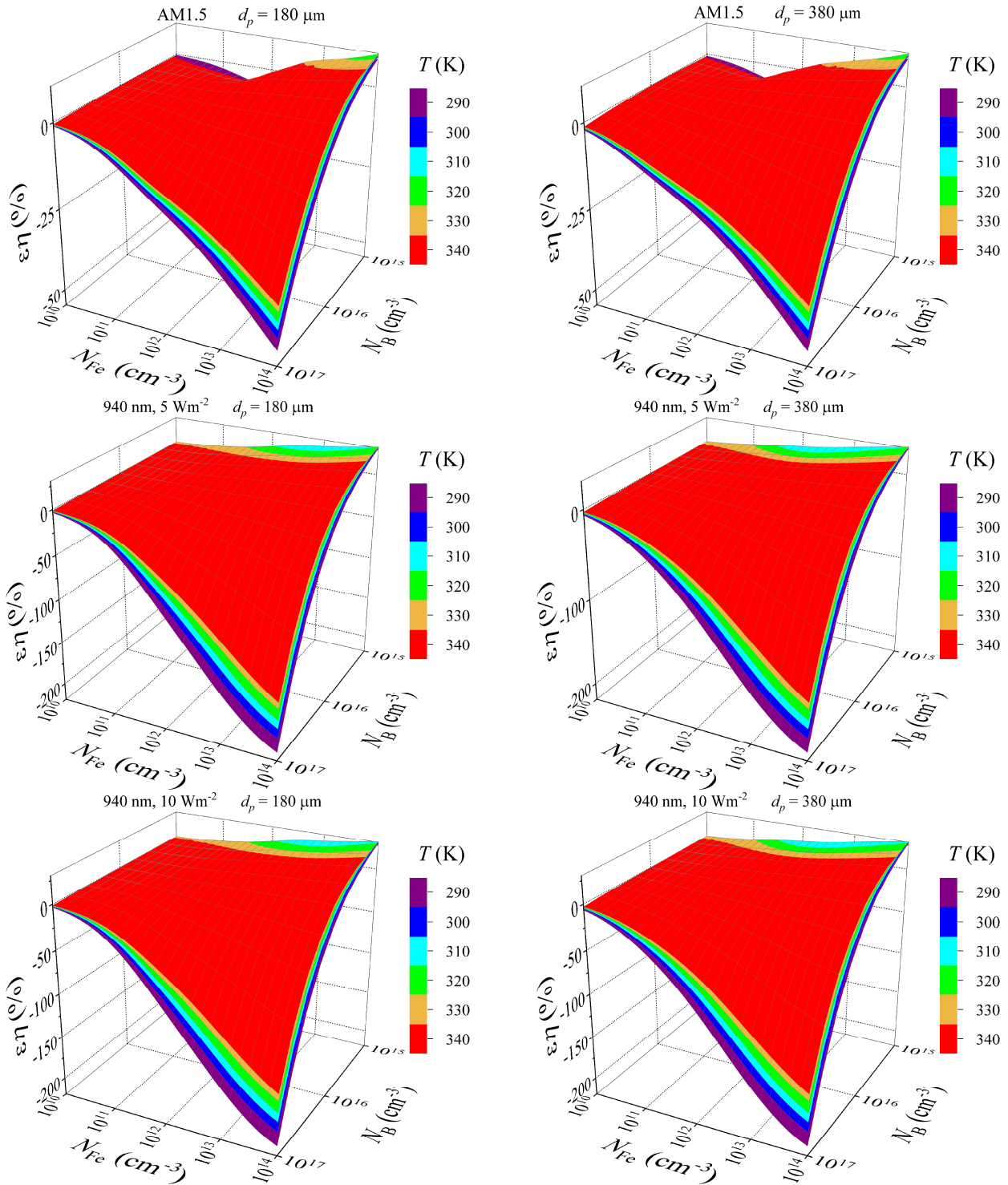


Fig.S18. Relative changes efficiency caused by a complete dissociation of  $\text{Fe}_\beta\text{B}_\alpha$  pairs as a function of iron concentration and doping level at different temperatures.  $d_p$ ,  $\mu\text{m}$ : 180 (left panels), 380 (right panels).

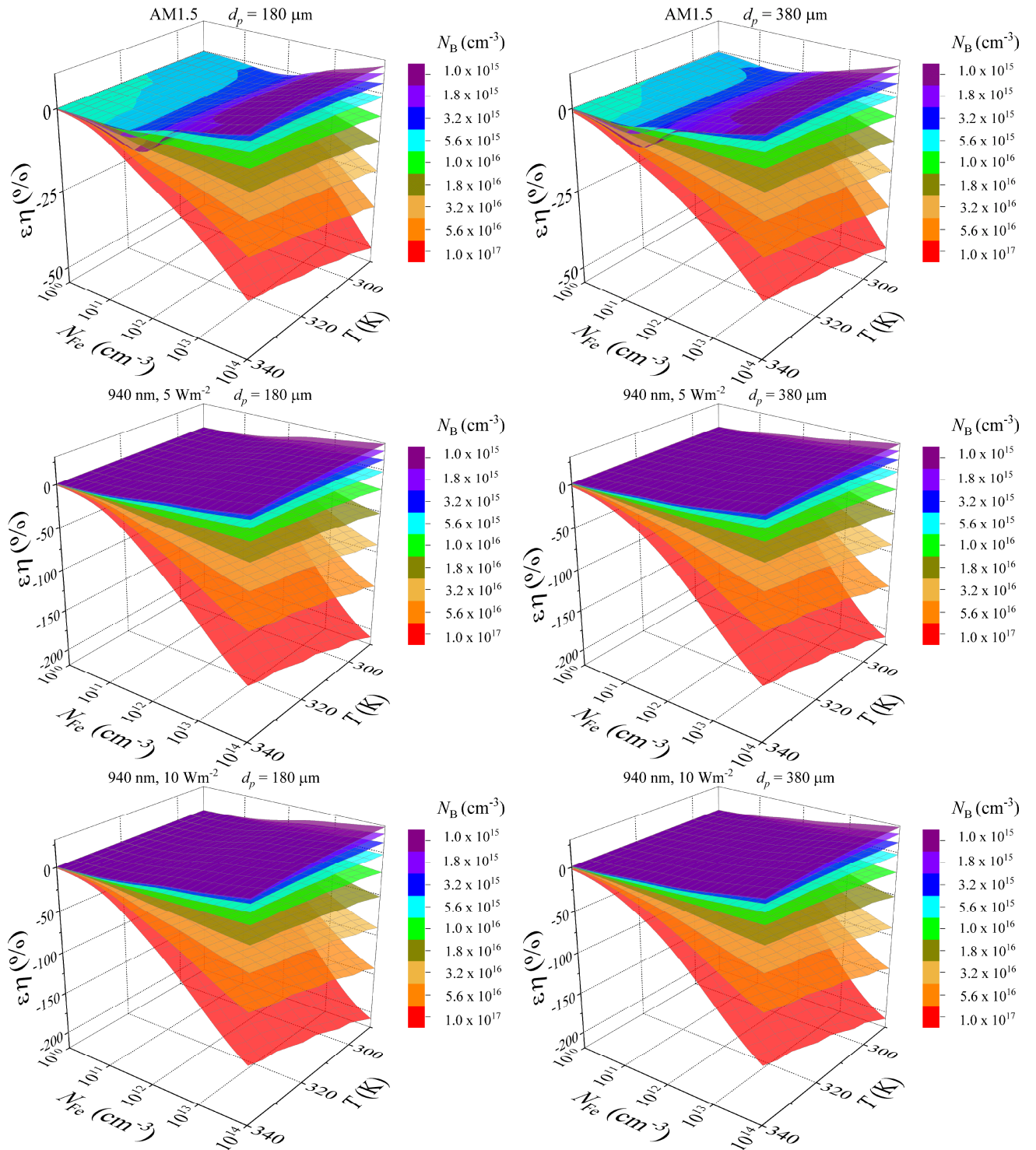


Fig.S19. Relative changes in efficiency caused by a complete dissociation of  $\text{Fe}_i\text{B}_s$  pairs as a function of iron concentration and temperature for SC with different base doping level.  $d_p$ ,  $\mu\text{m}$ : 180 (left panels), 380 (right panels).

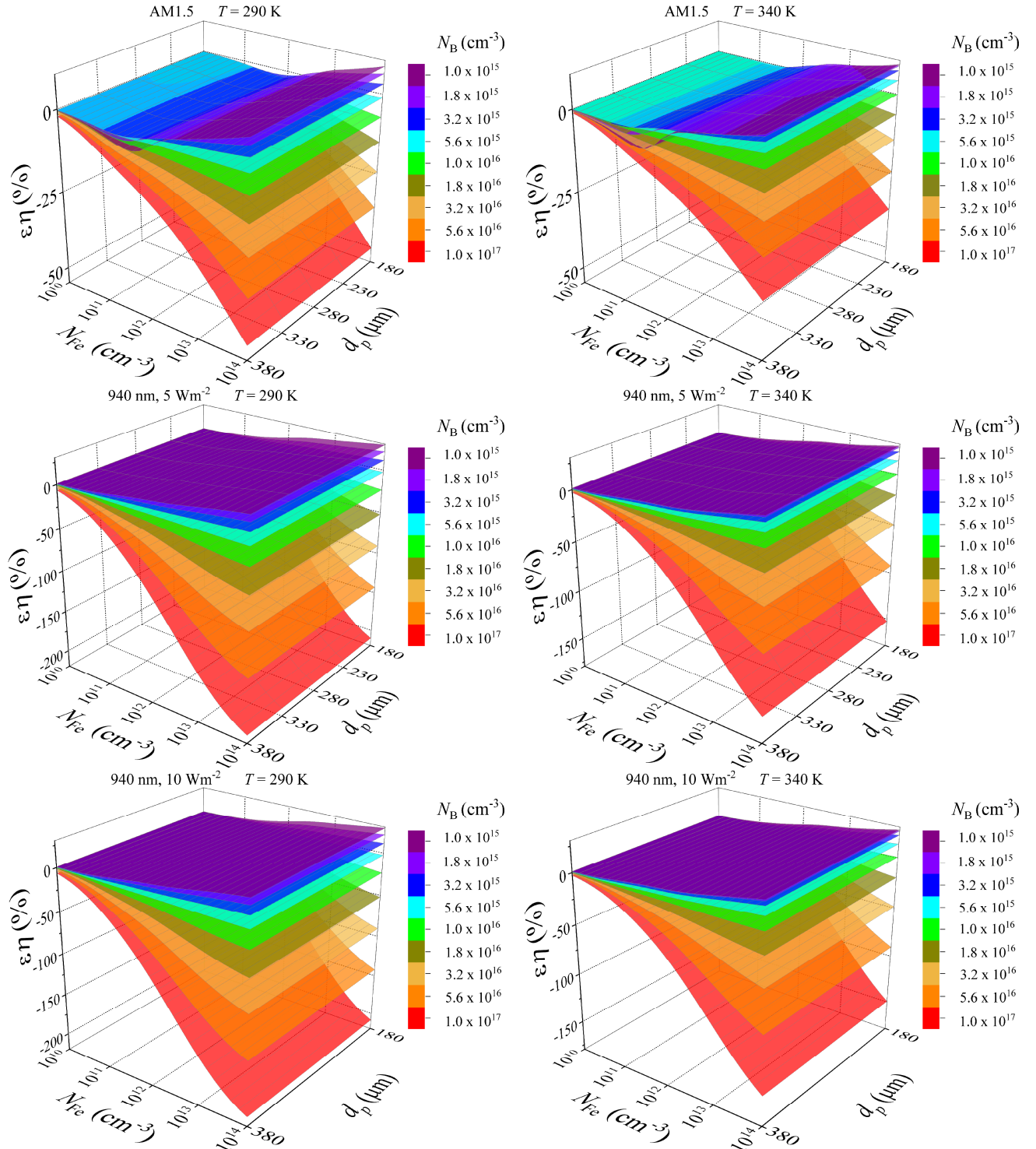


Fig.S20. Relative changes in efficiency caused by a complete dissociation of  $\text{Fe}_i\text{B}_s$  pairs as a function of iron concentration and base depth for SC with different base doping level.  $T, \text{K}$ : 290 (left panels), 340 (right panels).